# Freezing of Water Confined at the Nanoscale

F. G. Alabarse,[1] J. Haines,[1] O. Cambon,[1] C. Levelut,[2] D. Bourgogne,[1] A. Haidoux,[1] D. Granier,[1] and B. Coasne[1,*]

[1]*Institut Charles Gerhardt Montpellier, UMR—CNRS 5253, Université Montpellier 2 and ENSCM, Montpellier, France*

[2]*Laboratoire Charles Coulomb, Departement Colloides, Verres et Nanomateriaux, UMR—CNRS 5221 and Université Montpellier 2, Montpellier, France*

(Received 24 April 2012; published 18 July 2012)

Freezing of water in hydrophilic nanopores ($D = 1.2$ nm) is probed at the microscopic scale using x-ray diffraction, Raman spectroscopy, and molecular simulation. A freezing scenario, which has not been observed previously, is reported; while the pore surface induces orientational order of water in contact with it, water does not crystallize at temperatures as low as 173 K. Crystallization at the surface is suppressed as the number of hydrogen bonds formed is insufficient (even when including hydrogen bonds with the surface), while crystallization in the pore center is hindered as the curvature prevents the formation of a network of tetrahedrally coordinated molecules. This sheds light on the concept of an ubiquitous unfreezable water layer by showing that the latter has a rigid (i.e., glassy) liquidlike structure, but can exhibit orientational order.

DOI: 10.1103/PhysRevLett.109.035701 PACS numbers: 64.60.−i, 05.70.−a, 61.46.−w

Freezing of fluids confined at the nanoscale is of fundamental interest for the understanding of the effect of confinement, reduced dimensions, and surface forces on the behavior of fluids [1]. Shifts in the freezing point and, in some cases, new surface or confinement-induced phases are observed on reducing the diameter of the confined space to the range of the intermolecular forces. Among confined fluids, the freezing of water in pores is of utmost importance in chemistry, geology, biology, physics, etc. and is relevant to applications ranging from nanotribology [2], catalysis and phase separation [3], fabrication of nanomaterials using ice-templating [4], and the durability of concrete [5]. Experiments on ordered porous silica [6–9] have shown that water in the inner region of the pores crystallizes at a temperature $T_f$ below the bulk freezing point and which depends on the pore size $H$ according to the Gibbs-Thomson equation. In contrast, water molecules at the pore surface remain liquidlike as they are in strong interaction with the silica surface (through hydrogen bonding with silanol groups) so that they cannot participate in the formation of an icelike network of hydrogen bonds (HB). For hydrophobic nanopores, De Benedetti and coworkers [10] and others [11,12] have shown that, for temperatures below the bulk freezing point, water confined at high pressures crystallizes. Such crystallization in the case of hydrophobic surfaces is consistent with the work by Koga, Zeng, and Tanaka, who observed the formation of ice nanotubes in carbon nanotubes [12]. Owing to its specific nature, the results above for water depart from what is expected for simple fluids in nanopores of an ideal geometry [1]; i.e., $T_f$ is increased (decreased) compared to the bulk when the ratio of the fluid wall to the fluid-fluid interaction strengths is larger (smaller) than 1 (with $|\Delta T_f| \sim 1/H$). In contrast, the above results for water suggest that water crystallizes in hydrophobic pores while it remains liquidlike in hydrophilic pores. To shed light on the crystallization of water confined at the nanoscale, we report here a joint experimental and simulation study on the freezing of water in the cylindrical hydrophilic pores ($D = 1.2$ nm) of an aluminophosphate microporous crystal, $AlPO_4$-54. Using an optimized sol-gel route followed by hydrothermal treatment [13,14], we prepared an $AlPO_4$-54 single crystal of high quality which allows the ordering of confined water to be determined precisely using x-ray diffraction. The vibrational properties of nanoconfined water were investigated using Raman spectroscopy. Our results are also discussed in the light of Monte Carlo and molecular dynamics simulations which allow the structure and dynamics of water in $AlPO_4$-54 to be probed at the microscopic scale (the experimental and computational methods are described in Supplemental Material [15]). The present work adds to the knowledge of crystallization of nanoconfined water by reporting a picture that has not been observed previously; while the pore surface induces crystal-like orientational order of water in contact with it, water does not crystallize at temperatures $T$ as low as 173 K due to important confinement and surface effects on the number of hydrogen bonds and tetrahedral order of water. Of interest for freezing of nanoconfined liquids, this sheds light on the concept of an ubiquitous unfreezable adsorbed layer by showing that the latter has a rigid (i.e., glassy) liquidlike structure but can exhibit significant orientational order.

The crystal structure of hydrated $AlPO_4$-54 at $T = 293$, 235, and 173 K was refined (the structure found in [16] was used as a starting model). Introducing twinning on the (100) face in the refinement reduced the $R$ factor by 4%. The $R$ factor further decreased by 0.7% upon passing from an ordered model for confined water to a disordered model with a constant occupancy of 50%. The final $R$ factors and

 

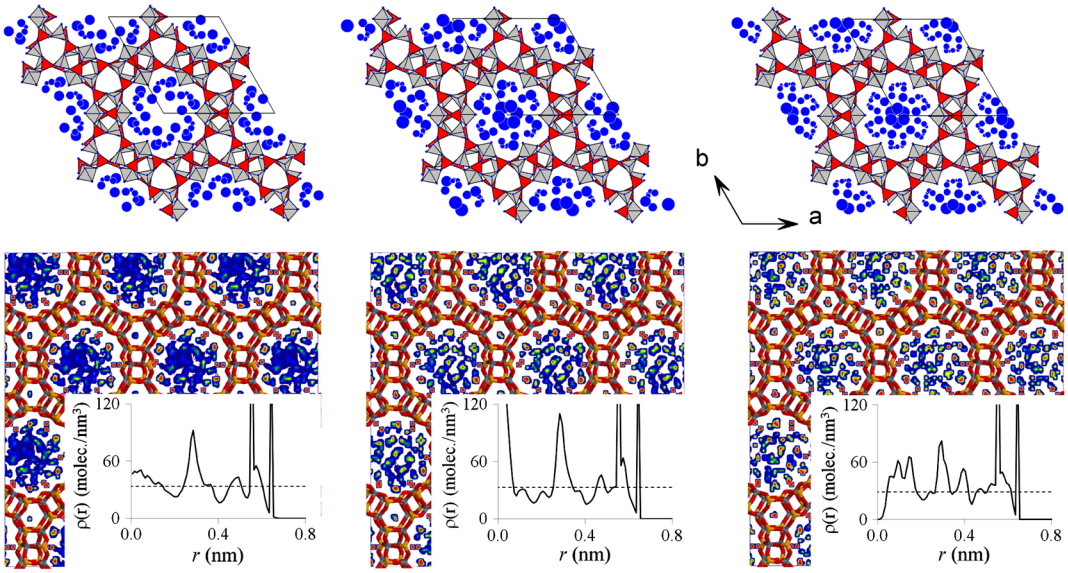


FIG. 1 (color online). Experimental (top) and simulated (bottom) structures of water in $AlPO_4$-54 at (left) 293 K, (center) 235 K, and (right) 173 K. The gray and red polyhedra in the experimental data are the $AlO_4$, $AlO_6$, and $PO_4$ units of $AlPO_4$, respectively, while the blue circles indicate the O of water (the ADP are represented at 50% probability). The simulated data are density maps of water in $AlPO_4$-54. The density scale increases linearly from purple, blue, green, yellow, orange, and red. The solid line in the inset shows the radial density for confined water with respect to the pore center, while the dashed line is the bulk density.

structural data [fractional atomic coordinates, atomic displacement parameters (ADP), bond lengths and angles] are given in Tables S3–S7 of the Supplemental Material [15]. $R_{eq}$, $R_{sigma}$, and agreement factors of the refinement are much lower than in previous work indicating that our $AlPO_4$-54 crystal is of very high quality. At all $T$ studied in this work, a few water molecules (OW1 and OW2) have low ADP similar to that for the atoms of $AlPO_4$. This result, which suggests that these molecules are in such a strong interaction with the $AlPO_4$ that they are nearly immobile, is in agreement with *ab initio* calculations in which a few water molecules were found to be framework molecules connected to $AlPO_4$ [17]. Based on these results, the center of mass of OW1 and OW2 were frozen in the simulations reported in this work. Figure 1 shows the experimental and simulated structures of water in $AlPO_4$-54 at $T = 293$, 235, and 173 K. The experimental structures show the $AlO_4$, $AlO_6$, and $PO_4$ tetrahedra and the positions of the O atoms of water (circle size represents the water O ADP at 50% probability). The simulated structures correspond to density maps of the O atoms of water. For each $T$, we also show the simulated radial density profile for water with respect to the pore center. Both the experimental and simulated data show that water ordering and site occupancies are more marked as $T$ decreases. This result is confirmed by the decrease in the experimental ADP upon cooling, especially for molecules in the vicinity of the pore surface (Tables S4–S5 given in Supplemental Material [15]). For all $T$, molecules close to the pore surface occupy well defined sites as revealed by marked density points in the experimental and simulated structures. As shown below, these sites are located in positions where water forms HB with the O atoms of $AlPO_4$-54. At low $T$, molecules in the pore center also occupy well defined positions due to lower thermal motion. In contrast, at $T = 293$ K, water in the pore center occupies the pore in a homogeneous way (as indicated by the absence of marked density in the experimental and simulated structures). This shows that water in the pore center is mobile enough at high $T$ so that it does not occupy well defined sites.

To probe the nature of confined water, Fig. 2 compares the experimental Raman spectra for water in $AlPO_4$-54 at 173 K, 235 K and 293 K and those for bulk ice and water. At 293 K, the Raman spectra for confined and bulk water are similar, as expected from the structure of confined

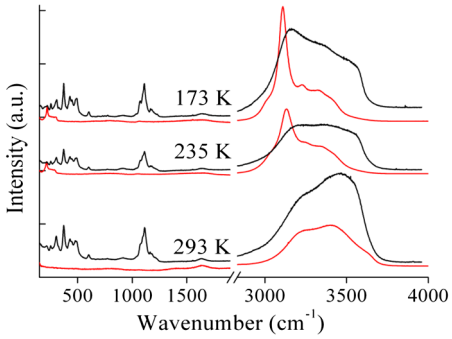


FIG. 2 (color online). Raman spectra for bulk water (red line) and water in $AlPO_4$-54 (black line). The water stretching bands has been multiplied by 0.2 for the sake of clarity.

water which remains mobile at this temperature. At lower $T$, the Raman spectra for bulk water are drastically modified as water crystallizes; a strong band at the lowest OH stretching frequency ($\sim 3130\ \mathrm{cm}^{-1}$) and a peak at low frequency ($\sim 220\ \mathrm{cm}^{-1}$) appear. In contrast, confined water does not crystallize at very low $T$ as the Raman spectra do not resemble those for ice. This result suggests that confined water does not crystallize despite the significant order of water in the vicinity of the $AlPO_4$ surface. To further characterize the structure of confined water, Fig. 3 shows the simulated pair correlation function $g(r)$ for water in $AlPO_4$-54 at different $T$. Both the $g(r)$ between the H and O of water and the H of water and the O of $AlPO_4$-54 were calculated. The peaks at $r < 0.2$ nm show that both HB between water molecules and between water and the $AlPO_4$-54 are observed. Due to the large charge $q = -1.2e$ carried by the O of $AlPO_4$-54, HB with the $AlPO_4$ surface are shorter (0.15 nm) than between water molecules (0.18 nm).

To further study possible formation of ice in $AlPO_4$-54, we investigated the structure of confined water in terms of number of HB and local order parameters. Based on the $g(r)$ functions, we assumed that HB between water molecules is such that the distance $dO_wH_w < 0.235$ nm while HB with $AlPO_4$-54 is such that $dOH_w < 0.225$ nm (in both cases the angle $\langle O_jO_iH_i \rangle$ must be lower than 30°). We also calculated the order parameter $q$, which quantifies the tetrahedrality of water [18]:

$$q_i = 1 - \frac{3}{8}\sum_{j=1}^{3}\sum_{k=j+1}^{4}\left[\cos(\psi_{kj}) + \frac{1}{3}\right]^2, \qquad (1)$$

where $\psi_{kj}$ is the angle formed by the segments joining the O atom of the water molecule $i$ and the O atoms of the nearest neighbor molecules $j$ and $k$. We included as possible nearest neighbors the O atoms of $AlPO_4$-54 to consider possible tetrahedral order formed with the host matrix. $q = 1$ for hexagonal ice (perfect tetrahedrality) while $q = 0.597$ for liquid water. We also calculated the orientational order parameter $q_{0,n} = \langle |\sum_j \exp(in\theta_j)|^2/N^2 \rangle$ where $n$ was varied from 1 to 20. Figure S3 in the Supplemental Material [15] shows $q_{0,n}$ for water in $AlPO_4$-54 at different $T$. We show $q_{0,n}$ for water in the pore center $r < 0.3$ nm, in the intermediate region $0.3\ \mathrm{nm} < r < 0.5$ nm, and in the contact layer $r > 0.5$ nm. While water in the central and intermediate regions does not exhibit orientational order, water in the contact layer exhibits 12-fold orientational order ($q_{0,12} = 0.6$), which is imposed by the symmetry of the O atoms in $AlPO_4$-54. Figure 4 shows the total number of HB as a function of the distance from the pore center. We report the contributions from water HB and from HB with the $AlPO_4$-54 surface (the latter is ~16% of the total number of HB). Figure 4 also shows $q$ as a function of the distance $r$ from the pore center. At 293 K, the number of HB in the pore center is close to the bulk value ($n_{OH} \sim 3.65$) while it is lower than the bulk close to the pore surface (as HB with the $AlPO_4$ does not counterbalance the decrease in water HB in this region due to steric repulsion). At low $T$, close to the pore surface, the number of HB remains too low to observe ice formation ($n_{OH} = 4$ for bulk ice). The latter result suggests that crystallization at the pore surface is hindered due to the solid surface that prevents the formation of a sufficient number of HB. In contrast, while the number of HB formed in the pore center is close to that for ice, crystallization is not observed in this region because curvature prevents tetrahedral ordering of the hydrogen bonded water molecules (even at low $T$, $q \sim 0.6$ in the pore center is close to the value for liquid water). The suppression of crystallization is supported by the fact that the $g(r)$ functions for confined water are nearly insensitive to $T$. Even for the water layer at the pore surface, 2D pair correlations functions $g(r)$, which are obtained by cutting the layer along the $z$ axis and unrolling it flat, are independent of $T$ (inset in

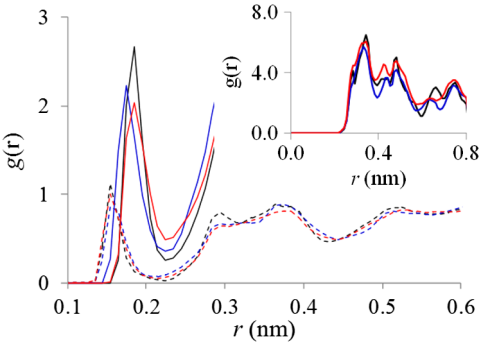


FIG. 3 (color online). $g(r)$ function for water in $AlPO_4$-54: 173 K (black), 235 K (blue), and 293 K (red). The solid and dashed lines are $g(r)$ functions between the H and O of water and the H of water and the O of $AlPO_4$-54. The inset shows the 2D $g(r)$ function for water in contact with the host surface.

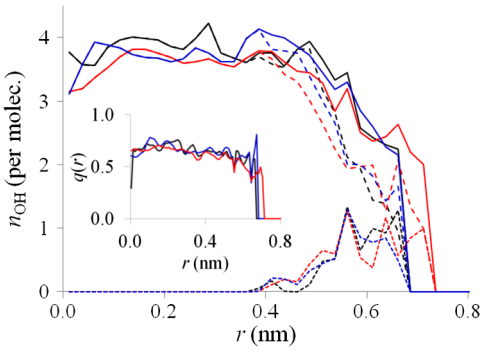


FIG. 4 (color online). Number of HB as a function of the distance from pore center for water in $AlPO_4$-54: 173 K (black data), 235 K (blue data), and 293 K (red data). The solid line is the total number of HB, while the dashed and dotted lines are the contributions arising from water HB and HB with the $AlPO_4$-54 surface, respectively. The inset shows the radial profile of the tetrahedral order parameter $q(r)$.

Fig. 3). On the other hand, the results above suggest that, despite the lack of crystallization, water in the vicinity of the surface can exhibit significant orientational order. This is consistent with the experimental ADP; the O atoms of water furthest away from the pore center at 173 K have similar ADP to those of the O atoms in ice [19], whereas the ADP increase towards the center.

To confirm the lack of crystallization of confined water, we studied its dynamics. Figure S4 in the Supplemental Material [15] shows the mean square displacements $\Delta r^2$ and correlation function $C(t) = \langle \cos\theta(t) \rangle$ for water in $AlPO_4$-54 and bulk water at 293, 235, and 173 K. $\theta(t)$ is the angle between a water OH bond at a time 0 and a time $t$. $\Delta r^2$ and $C(t)$ show that confined water is much slower than the bulk. At 293 K, the self-diffusivity $D_w = 2.4 \times 10^{-11}$ m$^2$/s of confined water, which was estimated from $\Delta r^2$ in the Fickian regime, is much lower than for bulk liquid water ($1.1 \times 10^{-9}$ m$^2$/s). At $T = 173$ and 235 K, $D_w \lesssim 10^{-13}$ m$^2$/s, which suggests that water is in a glassy state ($D_w$ for the liquid at such low $T$ would be 10 to 100 times larger). Figure S5 in the Supplemental Material [15] shows the absolute displacement $\Delta r$ and change in the orientation $\Delta\theta$ over a time step of 1 ps as a function of the distance to the pore center for water in $AlPO_4$-54. For all $T$, $\Delta r$ is smaller than for bulk water and decreases as the water approaches the surface. In contrast, $\Delta\theta$, which is less sensitive to the distance to the pore surface, is close but larger than for ice at low $T$. This result is fully consistent with previous neutron scattering and NMR experiments in which water at the surface was found in a state of reduced translation but enhanced rotation [20]. These results confirms that, despite the orientational order of water at the pore surface, water confined at low temperature is in a glassy state (rigid disordered structure with very slow dynamics). This study sheds light on the freezing of nanoconfined water by showing a situation that has not been observed previously. Both our experiments and simulations show that, despite the orientational order of water at the pore surface, water does not crystallize. Crystallization at the pore surface is suppressed because the number of HB formed is insufficient (even when considering hydrogen bonding with the host solid) while crystallization in the pore center is hindered because curvature effects prevent the formation of a network of tetrahedrally coordinated molecules. Given the pore size in $AlPO_4$-54, the lack of crystallization in the pore core is consistent with the Gibbs-Thomson equation [20]. The correct picture of freezing in the specific case considered here is an adsorbed layer of water molecules with crystal-like orientational order (imposed by the hydrophilic $AlPO_4$ surface) but positional disorder and a cylindrical core of glassy water in the pore center. In contrast to what is observed for large pores, freezing does not occur in the core region as the frustration arising from the curvature in such small nanopores is too strong. Although this hindrance effect of the cylindrical geometry has been reported for simple fluids, crystallization was, however, observed [21,22]. This study shows that strong curvature acts similarly as pore morphological and surface disorder [23] in preventing crystallization (again, despite ice-like orientational order of water at the surface). Despite the specific nature of water (hydrogen bonding, high dielectric constant), the present experimental and simulation approach can be used to look at the competition between geometrical frustration and surface-induced order for other fluids.

We thank O. Torno (Sasol Germany Gmbh) for providing the Pural SB. Support from the Agence Nationale de la Recherche is acknowledged (ANR-09-BLAN-0018-01).

*benoit.coasne@ensm.fr

[1] C. Alba-Simionesco, B. Coasne, G. Dosseh, G. Dudziak, K. E. Gubbins, R. Radhakrishnan, and M. Sliwinska-Bartkowiak, J. Phys. Condens. Matter **18**, R15 (2006).
[2] J. Klein and E. Kumacheva, Science **269**, 816 (1995).
[3] L. D. Gelb, K. E. Gubbins, R. Radhakrishnan, and M. Sliwinska-Bartkowiak, Rep. Prog. Phys. **62**, 1573 (1999).
[4] S. Deville, E. Saiz, and R. K. Nalla, Science **311**, 515 (2006).
[5] O. Coussy, *Mechanics and Physics of Porous Solids* (Wiley, New York, 2010).
[6] R. Schmidt, E. W. Hansen, M. Stoecker, D. Akporiaye, and O. H. Ellestad, J. Am. Chem. Soc. **117**, 4049 (1995).
[7] A. Schreiber, I. Ketelsen, and G. H. Findenegg, Phys. Chem. Chem. Phys. **3**, 1185 (2001).
[8] K. Morishige and H. Iwasaki, Langmuir **19**, 2808 (2003).
[9] M. Sliwinska-Bartkowiak, M. Jazdzewska, L. L. Huang, and K. E. Gubbins, Phys. Chem. Chem. Phys. **10**, 4909 (2008).
[10] N. Giovambattista, P. J. Rossky, and P. G. De Benedetti, J. Phys. Chem. **113**, 13 723 (2009).
[11] R. Zangi and A. E. Mark, J. Chem. Phys. **119**, 1694 (2003).
[12] K. Koga, X. C. Zeng, and H. Tanaka, Phys. Rev. Lett. **79**, 5262 (1997); K. Koga, G. T. Gao, H. Tanaka, and X. C. Zeng, Nature (London) **412**, 802 (2001).
[13] J. O. Martinez, C. Falamaki, C. Baerlocher, and L. B. McCusker, Microporous Mesoporous Mater. **28**, 261 (1999).
[14] E. Jahn, D. Mueller, and J. Richter-Mendau, in *Synthesis of Microporous Materials*, edited by M. L. Occelli and H. Robson (Van Nostrand Reinhold, New York, 1992), p. 248.
[15] See Supplemental Material at http://link.aps.org/supplemental/10.1103/PhysRevLett.109.035701 for experimental and computational methods and additional structural, order parameter, and dynamical data.
[16] G. Cheetham and M. M. Harding, Zeolites **16**, 245 (1996).
[17] G. Poulet, A. Tuel, and P. Sautet, J. Phys. Chem. B **109**, 22 939 (2005).
[18] A. K. Soper and C. J. Benmore, Phys. Rev. Lett. **101**, 065502 (2008).
[19] W. F. Kuhs and M. S. Lehman, J. Phys. Chem. **87**, 4312 (1983).

[20] B. Webber and J. Dore, J. Phys. Condens. Matter **16**, S5449 (2004); J. B. W. Webber, Prog. Nucl. Magn. Reson. Spectrosc. **56**, 78 (2010).
[21] M. W. Maddox and K. E. Gubbins, J. Chem. Phys. **107**, 9659 (1997).
[22] M. Sliwinska-Bartkowiak, G. Dudziak, R. Sikorski, R. Gras, R. Radhakrishnan, and K. E. Gubbins, J. Chem. Phys. **114**, 950 (2001).
[23] B. Coasne, S. K. Jain, and K. E. Gubbins, Phys. Rev. Lett. **97**, 105702 (2006).